ACS APPLIED MATERIALS & INTERFACES

Research Article

www.acsami.org

An Efficient Mono-Component Polymeric Intumescent Flame Retardant for Polypropylene: Preparation and Application

Zhu-Bao Shao, Cong Deng,* Yi Tan, Ming-Jun Chen, Li Chen, and Yu-Zhong Wang*

Center for Degradable and Flame-Retardant Polymeric Materials, College of Chemistry, State Key Laboratory of Polymer Materials Engineering, National Engineering Laboratory of Eco-Friendly Polymeric Materials (Sichuan), Analytical and Testing Center, Sichuan University, Chengdu 610064, China

ABSTRACT: We found in our previous study that ethylenediamine- or ethanolamine-modified ammonium polyphosphates could be used alone as an intumescent flame retardant for polypropylene (PP), but their flame-retardant efficiency was not very high. In this present work, a novel highly-efficient mono-component polymeric intumescent flame retardant, piperazine-modified ammonium polyphosphate (PA-APP) was prepared. The oxygen index value of PP containing 22 wt % of PA-APP reached 31.2%, which increased by 58.4% compared with that of PP with equal amount of APP, and the vertical burning test (UL-94) could pass V-0 rating. Cone calorimeter (CC) results indicated that PP/PA-APP composite exhibited superior performance compared with PP/APP composite. For PP containing 25 wt % of PA-APP, fire growth rate (FGR) and smoke production rate (SPR) peak were reduced by 86.4% and 78.2%, respectively, compared with PP blended with 25 wt % APP. The relevant flame-retardant mechanism of PA-APP was investigated by Fourier transform infrared spectroscopy etc. The P−N−C structure with the alicyclic amine was formed during the thermal decomposition of piperazine salt (−NH_2^+−O−P−), and the rich P−N−C structure facilitated the formation of stable char layer at the later stage, consequently improving the flame-retardant efficiency of APP.

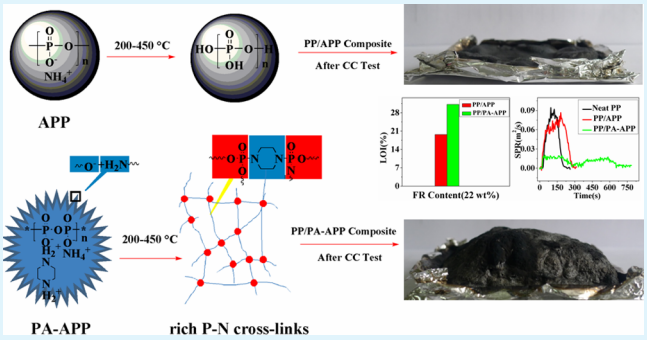

KEYWORDS: *ammonium polyphosphate, piperazine, flame retardant, polypropylene*

1. INTRODUCTION

Some halogen-free flame retardants, such as aluminum hydroxide, magnesium hydroxide, metal borates, intumescent flame retardants (IFR), etc., have been applied to prepare the flame-retard PP composites.[1−5] In these halogen-free flame retardants, IFR and metal hydroxide have been proved to be very effective to flame retard PP compared with the other halogen-free flame retardants.[3,5,6] For metal hydroxide, the loading is quite high to achieve the good flame retardancy of PP, generally above 50 wt %,[6−8] which inevitably brings some concomitant shortcomings.[9,10] However, the same flame-retardant efficiency can be achieved at much lower loading for IFR, and the negative impacts of IFR are also much lower than those of metal hydroxide on the other properties of PP, due to the low loading of IFR in polymer matrix.[11] On the basis of the advantages of IFR in flame retarding PP, the research on IFR has become a hot issue at present.

Generally, IFR mainly contains three components, which are acid source, blowing agent, and charring agent. In most cases, APP is chosen as acid source and blowing agent in IFR.[12] As we know, the flame-retardant efficiency on PP is quite low when APP is used alone.[13,14] To achieve the efficient intumescent flame retardation in polymer, charring agent is necessary to form an expanded char layer during the combustion. A simple method is that APP is used together with an additional charring agent. However, many charring agents have still different shortcomings, for instance, low flame-retardant efficiency,[15] a complicated preparation process,[16−18] harm to the environment,[5,19] etc. To overcome these disadvantages, an ideal pathway should be to develop a flame retardant that can combine all the three characteristics of IFR mentioned above. APP derivatives should be one of the best candidates, because APP gathers two characteristics: acid source and blowing agent.

In our previous paper,[20] a chemical method used to prepare the modified APP was reported, in which APP modified through ethylenediamine (EDA) or ethanolamine (ETA) was incorporated into PP to improve its flame retardation. The results showed that the oxygen index(OI) value of PP/EDA-APP reached 29.5%, and the V-0 rating was achieved at the loading of 30 wt % EDA-APP. Obviously, the loading of EDA-APP is not very low to reach the UL-94 V-0 rating and high OI value, so it is necessary to develop some more efficient APP derivatives to flame retard PP.

In present work, a novel kind of mono-component polymeric intumescent flame retardant, PA-APP, was prepared by chemically-incorporating piperazine in APP molecular chains,

Received: February 6, 2014
Accepted: April 17, 2014
Published: April 17, 2014

   dx.doi.org/10.1021/am500789q | ACS Appl. Mater. Interfaces 2014, 6, 7363−7370

and characterized by FTIR, ^{1}H-NMR, XPS, and XRD. The resulting PA-APP was added into PP to improve the flame retardancy. The flame retardancy of PP/PA-APP and the flame-retardant mechanism were investigated with the aid of different measurements.

2. EXPERIMENTAL SECTION

2.1. Materials. Commercial APP (form II) with a degree of polymerization of 900-1100 was supplied by Taifeng New-Type Flame Retardants Co., Ltd. (Shifang, China); piperazine (AR) and ethanol (AR) were purchased from Tianjin Kemiou Chemical Reagent Co., Ltd. (Tianjin, China); polypropylene (T30S) was obtained from Petro China Lanzhou Petrochemical Co., Ltd. (Lanzhou, China).

2.2. Measurements. The average sizes of APP and PA-APP particles were detected by Master Sizer 2000 (Malvern Instruments Ltd., UK) at room temperature.

FTIR spectra were recorded by a Nicolet FTIR 170SX spectrometer (Nicolet, America) using the KBr disk, and the wave number range was set from 4000−500 cm^{-1}.

^{1}H-NMR spectra were recorded on a Bruker AV II-400 MHz spectrometer (Bruker, Switzerland) by using D_2O as a solvent.

XRD patterns using Cu Kα radiation (λ = 1.542 Å) were performed with power DX-1000 diffractometer (Dandong Fangyuan, China) at the scanning rate of 0.02° per second in the 2θ range of 5−50°.

The surface morphologies of the APP and PA-APP were observed by using a JEOL JSM 5900LV scanning electron microscopy (SEM) (JEOL, Japan) at the accelerating voltage of 5 kV.

Tensile test was completed in accordance with the procedures in GB/T 1040.1-2006 at a crosshead speed of 20 mm/min. The Izod impact property was tested in accordance with the procedures in GB/T 1843-2008, and the depth of nick is 2 mm.

The contents of carbon (C) and nitrogen (N) in APP and PA-APP were measured by elemental analysis (EA) on CARLO ERBA1106 instrument (CarloErba, Italy).

OI value was measured using an HC-2C oxygen index instrument (Jiangning, China) according to ASTM D2863-97 with a sheet dimension of 130 mm × 6.5 mm × 3.2 mm.

UL-94 vertical burning level was tested on a CZF-2 instrument (Jiangning, China) according to ASTM D 3801; the dimension of samples is 130 mm × 13 mm × 3.2 mm.

The flammability of the sample was measured by a cone calorimeter device (Fire Testing Technology, UK). The samples with the dimension of 100 mm × 100 mm × 3 mm were exposed to a radiant cone at a heat flux of 50 kW/m^2.

Thermogravimetric (TG) analysis was carried out by a TG 209F1 (NETZSCH, Germany) thermogravimetric analyzer at a heating rate of 10 °C/min under the nitrogen flow of 50 mL/min with the temperature range from 40 to 700 °C.

XPS spectra were recorded by a XSAM80 (Kratos Co, UK), using Al K$_a$ excitation radiation ($h\nu$ − 1486.6 eV)

2.3. Preparation of PA-APP. A certain volume ratio of ethanol to water (700 mL/40 mL) was poured into a three-neck flask equipped with a stirrer under a nitrogen atmosphere. Half an hour later, piperazine (43 g) was injected into the flask and then stirred for about 10 min. When piperazine was dissolved in the mixed solution, 100 g APP was added into the flask. After that, the mixture was heated up to 90 °C which is the set reaction temperature. When the reaction was completed, pH test strip was used to detect whether there existed ammonia. If both pH values were about 8−9 at an interval of 10 min, meaning that the reaction completed. Next, the reaction mixture was cooled to room temperature. The white solid was then filtered and washed with ethanol, finally dried to a constant weight. The yield was about 80% in our experiment. The average sizes of APP and PA-APP particles were investigated, which are about 16.9 μm and 29.8 μm, respectively.

2.4. Sample Preparation. *2.4.1. Samples for the Combustion Test.* Both the commercial APP and the prepared PA-APP were dried in a vacuum oven at 80 °C for 12 h. Then the PP samples containing different ratios of APP or PA-APP were prepared via a twin-screw extruder (CTE 20, Kebeilong Keya Nanjing Machinery Co., Ltd, Nanjing, China) with the rotation speed of 150 rpm at the following temperature protocol from the feed zone to the die: 175, 180, 190, 185, 180, and 170 °C. Finally the extruded pellets were hot-pressed into different samples by plate vulcanizer (Qingdao Yadong Rubber machinery Co. Ltd. China).

2.4.2. Residual Char Samples for FTIR Test and XPS Test. The samples were heated to 200, 250, 330, 420, and 530 °C, respectively, at a heating rate of 10 °C/min under a nitrogen atmosphere in TG, and retained 10 min at these temperatures, then the residual char samples were obtained. Here, the choice of these temperatures is dependent on TG results of APP and PA-APP.

3. RESULTS AND DISCUSSION

3.1. Characterization of PA-APP. The FTIR spectra of PA-APP and APP are shown in Figure 1. For PA-APP, all the

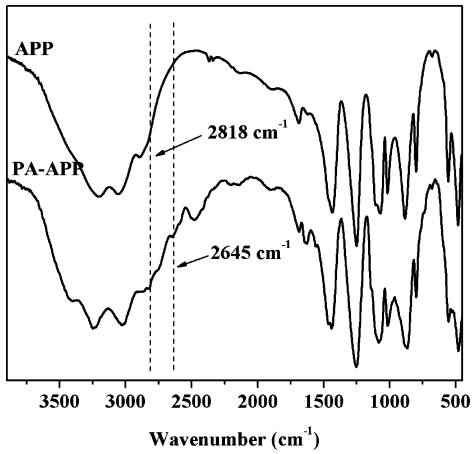

Figure 1. FTIR spectra of APP and PA-APP.

typical peaks of APP still exist. Moreover, some new absorption peaks appeared. The new weak peaks at 2818 and 2645 cm^{-1} are ascribed to the vibration of $-CH_2-$ and $-NH_2^+$, respectively. The appearance of the two peaks proves that the piperazine salt ($-NH_2^{+\cdot}O-P-$) might be formed after incorporating PA into APP. The peaks at 3400−3030 cm^{-1} are assigned to the NH_4^+ asymmetry stretching vibration,[21] indicating that part of NH_4^+ was still kept in PA-APP, which did not engage in the reaction between PA and APP.

To confirm the formation of chemically modified PA-APP, we performed the ^{1}H NMR test of APP, PA, the mixture of APP and PA (APP+PA), and PA-APP prepared through chemical method, and the results are presented in Figure 2. Here, it should be noted that all the peaks at 4.80 ppm in four figures are ascribed to the solvent "deuterated water". For APP (Figure 2a), there is only one peak at 4.80 ppm; Figure 2b shows that there is a new peak at 2.71 ppm besides the peak at 4.80 ppm, which corresponds to the $-CH_2-$ protons in PA; for APP+PA (Figure 2c), there are two peaks at 4.80 and 2.71 ppm, and the latter one is also ascribed to the $-CH_2-$ protons in PA. In the ^{1}H NMR spectrum of PA-APP, a new peak appeared at 3.59 ppm, which is ascribed to the $-CH_2-$ protons in $-CH_2-NH_2^+$, indicating the structure of piperazine salt was formed. In addition, there is no more peak other than the peaks at 3.59 and 4.80 ppm for PA-APP, meaning that no PA was left. All the results of ^{1}H NMR demonstrated that PA-APP was obtained successfully.

To further demonstrate the formation of PA-APP, we investigated XPS results of APP, PA, and PA-APP. Their N_{1s}

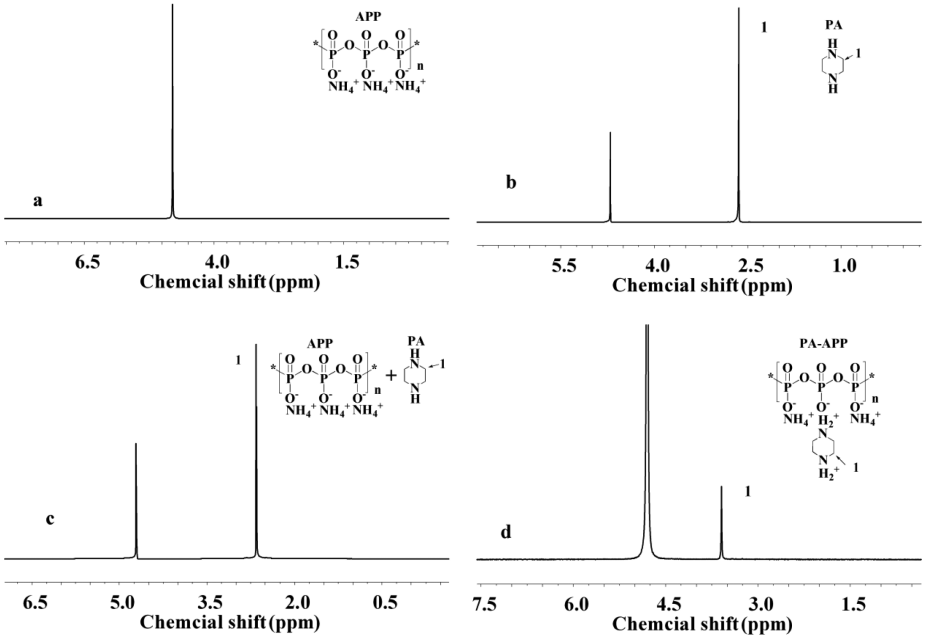

Figure 2. ^{1}H-NMR spectra of (a) APP, (b) PA, (c) APP+PA and (d) PA-APP.

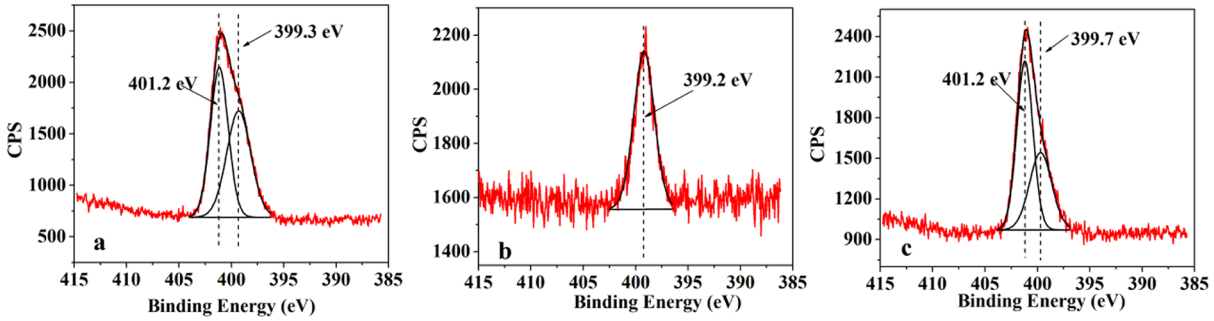

Figure 3. N_{1s} spectra of (a) APP, (b) piperazine, and (c) PA-APP.

spectra are shown in Figure 3. For APP, the binding energy at around 401.2 eV corresponds to NH_4^+, and the peak at 399.3 eV may correspond to the N(-P-NH-P-). The XPS result of APP is consistent with Camino's report.[22] For PA, the peak at around 399.2 eV is ascribed to the −C−NH−C−. After being chemically modified by PA, a new peak can be observed at 399.7 eV for PA-APP, which should be attributed to the N in $-C-NH_2^+-C-$, indicating that the structure of piperazine salt was formed after incorporating PA into APP.

In addition, EA test was used to confirm that the PA-APP was prepared successfully from another point of view. The carbon (C) and nitrogen (N) contents of APP and PA-APP are listed in Table 1. For APP, contents of the C and N were 0.40 and 13.8%, respectively. After incorporating the piperazine, the content of C increased to 9.90%, whereas the content of N reduced to 12.6%. The results also demonstrate that the PA-APP was obtained successfully.

Table 1. C and N Contents of APP and PA-APP

	C (%)	N (%)
APP	0.40	13.8
PA-APP	9.90	12.6

Finally, XRD illustrated that, compared with APP, the diffraction peaks of PA-APP almost appeared at the same positions, indicating that the crystalline structures of APP were not affected by the modification.

3.2. Mechanical Properties of Flame-Retardant PP Composites. Mechanical properties, including tensile strength, elongation at break, and impact strength are listed in Table 2. Compared with PP/APP composite, PP/PA-APP composite with equal amount of flame retardant has no apparent change in tensile strength, impact strength, and elongation at break. To investigate the effect of flame retardant on the mechanical properties, we performed SEM test of PP composites

Table 2. Mechanical Properties of PP/APP and PP/PA-APP

sample	flame retardant (wt %)	tensile strength (MPa)	elongation at break (%)	impact strength (kJ/m^2)
PP/APP	20	27.7 ± 0.2	90.1 ± 8.9	1.61±0.08
	25	25.0 ± 0.4	67.3 ± 8.2	1.73 ±0.07
	30	23.4±0.3	34.1 ± 5.7	1.75 ± 0.07
PP/PA-APP	20	27.0 ± 0.3	89.4 ± 9.4	1.65 ± 0.05
	25	25.6 ± 0.4	70.3 ± 7.5	1.70 ± 0.03
	30	23.2 ± 0.2	32.3 ± 6.5	1.78 ± 0.04

dx.doi.org/10.1021/am500789q | ACS Appl. Mater. Interfaces 2014, 6, 7363−7370

containing 25 wt % flame retardant to observe the dispersion of APP and PA-APP, and the results are shown in Figure 4. Most

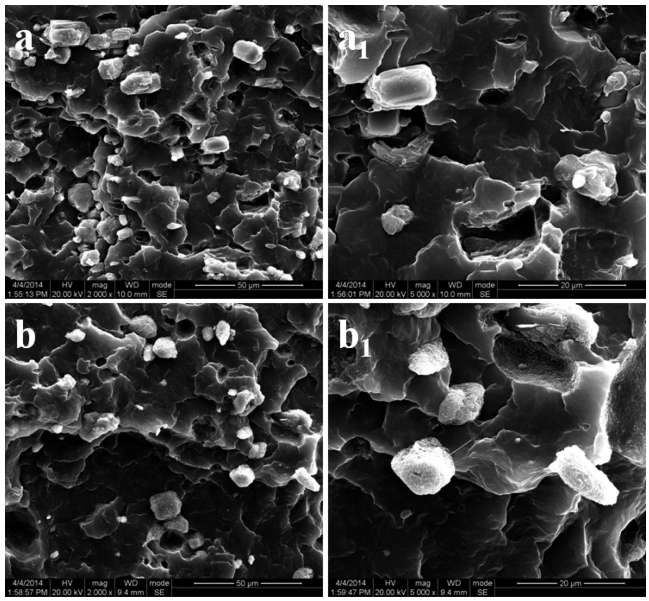

Figure 4. SEM micrographs of (a, a_1) PP/25 wt % APP and (b, b_1) PP/25 wt % PA-APP.

of APP or PA-APP particles were dispersed well in PP matrix, but a small amount of APP or PA-APP aggregates were formed for both PP composites. Obviously, both APP and PA-APP particles have similar dispersion and interface in PP, indicating that the chemical modification through PA did not apparently change the dispersion and interface of APP in PP matrix, which should be the reason for the little differences of mechanical properties between PP/APP and PP/PA-APP at the same loading of flame retardant.

3.3. Flame Retardancy. The OI and UL-94 tests are used to evaluate flame-retardant performances of neat PP, PP/APP, and PP/PA-APP composites, and the data are listed in Table 3.

Table 3. OI and UL-94 results of neat PP, PP/APP and PP/PA-APP composites

component (wt %)				UL-94 (3.2 cm)	
PP	APP	PA-APP	OI (%)	rating	dripping
100	0	0	18.0	NR	yes
80	20	0	19.5	NR	yes
78	22	0	19.7	NR	yes
75	25	0	20.0	NR	yes
70	30	0	20.4	NR	yes
80	0	20	29.5	V2	no
78	0	22	31.2	V0	no
75	0	25	32.5	V0	no
70	0	30	35.6	V0	no

The two tests show that neat PP is a flammable polymer. For PP/APP composite, the OI value increased slightly as more APP was added. When the loading was 22 wt %, the OI value of the PP/APP composite was 19.7%. With increasing APP to 30 wt %, the OI value of the PP/APP composite reached 20.4%, indicating that APP was not very effective to improve the flame retardancy of PP. On the other hand, with increasing the PA-APP, the OI value of PP/PA-APP composite increased significantly. At 22 and 30 wt % PA-APP, OI values of the PP/PA-APP composite reached 31.2 and 35.6%, respectively, which correspondingly increased by 58.4 and 74.5% compared with those of PP/APP with equal amount of flame retardant. So PA-APP is much more effective to improve the OI value of PP than APP.

PP/APP composite at a loading of 22 wt % showed no rating in UL-94 test, and had obvious dripping. However, when the content of PA-APP was 22 wt %, PP/PA-APP composite could pass UL-94 V-0 rating (3.2 mm) and the dripping was not observed. Furthermore, when the content of PA-APP increased to 30 wt %, the PP/PA-APP composite could pass UL-94 V-0 rating (1.6 mm) while PP/APP composite was still no rating at the same loading of flame retardant. So the flame-retardant efficiency of PA-APP is much higher than that of APP in UL-94 test.

CC is an effective method to assess flammability behavior of materials. Here, three typical systems were chosen to analyze the combustion behaviors in CC test, which are neat PP, PP/25 wt % APP, and PP/25 wt % PA-APP. The HRR, THR, SPR, and TSP curves of neat PP and PP composites are shown in Figures 5 and 6, and the corresponding data are presented in Table 4. It could be observed that neat PP burned rapidly, and its peak of HRR (PHRR) and THR were 841.6 kW/m^2 and 89.1 MJ/m^2, respectively. When incorporating 25 wt % APP into PP, the PHRR reduced to 473.3 kW/m^2, but the THR of PP/APP composite increased slightly to 90.2 MJ/m^2. After APP was modified through PA, both PHRR and THR of PP/25 wt % PA-APP decreased compared with the corresponding value of PP/25 wt % APP, especially for PHRR, which decreased to 162.6 kW/m^2, reduced by 65.6% compared with that of PP/APP.

On the basis of the HRR curves, fire growth rate (FGR) has been calculated to assess the fire hazard of the composite according to the following equation[23,24]

$$\mathrm{FGR} = \mathrm{PHRR}/t_{\mathrm{PHRR}}$$

Generally, a lower FGR value indicates that the time to flashover is delayed.[25] For PP/APP composite, the FGR decreased to 6.31 kW/(m^2 s) from 7.32 kW/(m^2 s). For PP/25 wt % PA-APP, the t_{PHRR} was 190 s, so the FGR of PP/PA-APP composite was 0.86 kW/m^2.s, which was greatly decreased by 86.4% compared with PP/APP composite. The result demonstrates that the incorporation of PA in APP greatly reduced the FGR of PP/APP composite, and consequently could significantly extend the time to escape in a real accident.

The SPR and TSP curves of neat PP and PP composites are presented in Figure 6, and the corresponding data are summarized in Table 4. It is clear that both APP and PA-APP could decrease the SPR, which decreased to 0.087 m^2/s for PP/APP and 0.019 m^2/s for PP/PA-APP, respectively, from 0.095 m^2/s for neat PP. Despite an improvement in SPR for PP/APP, its TSP value increased to 14.3 m^2 from 10.1 m^2 for neat PP. Noticeably, APP could not lower the TSP value. But for PA-APP, the TSP value decreased to 8.2 m^2, which is lower than that of neat PP obviously. These results illustrate that PA-APP restrained the production of smoke, while APP deteriorated the TSP of PP, demonstrating that the smoke suppression of PA-APP is more efficient than that of APP.

Table 4 shows that the average MLR of PP/APP composite is almost the same as that of neat PP, and they are 0.067 g/s and 0.065 g/s, respectively, but it decreases markedly for PP/25 wt % PA-APP, and the value is 0.023 g/s.

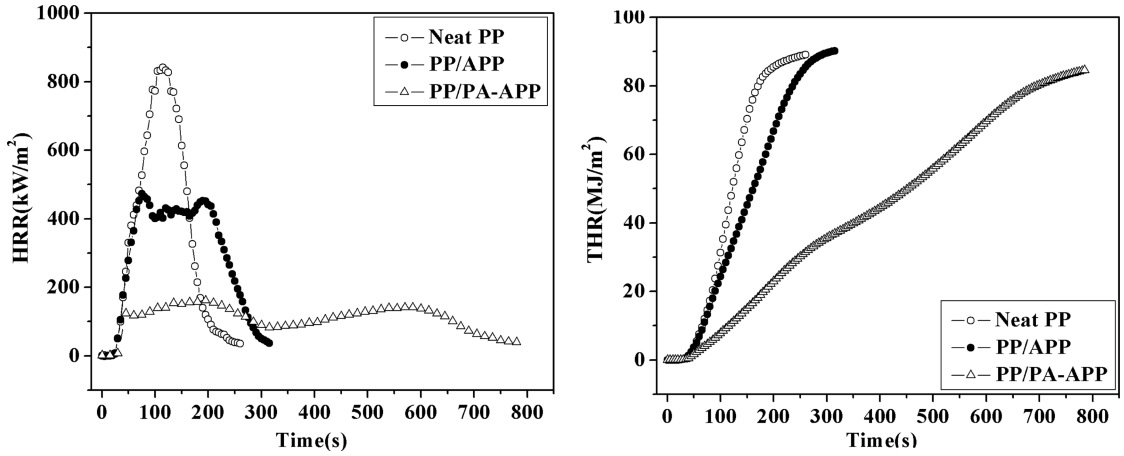

Figure 5. HRR and THR plots of neat PP, PP/25 wt % APP, and PP/25 wt % PA-APP composites.

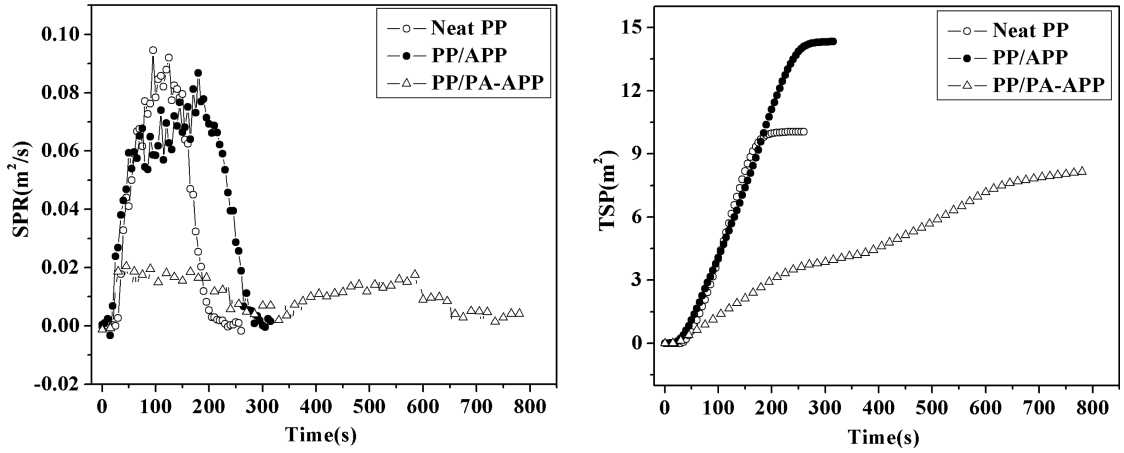

Figure 6. SPR and TSP curves of neat PP, PP/25 wt % APP, and PP/25 wt % PA-APP composites.

Table 4. CC Data of Neat PP, PP/APP, and PP/PA-APP Composites

sample	PP	PP/APP	PP/PA-APP
TTI (s)	25	13	17
PHRR (kW/m^2)	841.6	473.3	162.6
time to PHRR (s)	115	75	190
FGR (kW/(m^2 s))	7.32	6.31	0.86
THR (MJ/m^2)	89.1	90.2	84.5
peak SPR (m^2/s)	0.095	0.087	0.019
TSP (m^2)	10.1	14.3	8.2
average MLR (g/s)	0.067	0.065	0.023

The digital photos of the residues for neat PP, PP/APP, and PP/PA-APP composites after CC test are shown in Figure 7.Generally, the intumescent char layer could slow the heat and mass transfer between gas and condensed phases, and could also protect the underlying materials from further burning. So the formation of intumescent char layer should be the most important factor to achieve the much better flame retardancy of PP/PA-APP composite.

Figure 8 shows the SEM micrographs of the residue surfaces of PP/APP and PP/PA-APP composites after CC test. These micrographs further demonstrate the char layer of PP/PA-APP composite is much better that of PP/APP. As shown in Figure 8, the char layer left after being burnt is so thin for PP/25 wt % APP, and there are some obvious holes in the char layer.

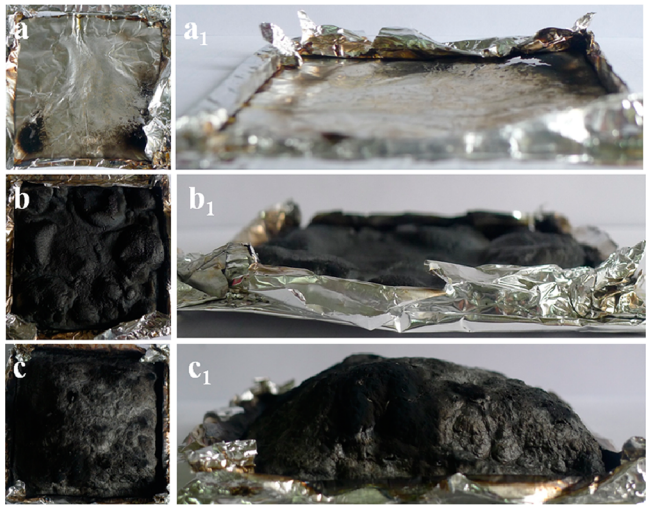

Figure 7. Digital photographs of residues of (a, a$_1$) neat PP, (b, b$_1$) PP/APP, and (c, c$_1$) PP/PA-APP composites after CC test.

However, the char layer for PP/PA-APP composite is more continuous and more compact. The char layer formed could effectively provide a barrier between PP/PA-APP composite and fire, and consequently protect the underlying materials.

3.4. Flame Retardant Mechanism of PA-APP. Figure 9 shows the thermal decomposition curves of APP and PA-APP

dx.doi.org/10.1021/am500789q | ACS Appl. Mater. Interfaces 2014, 6, 7363−7370

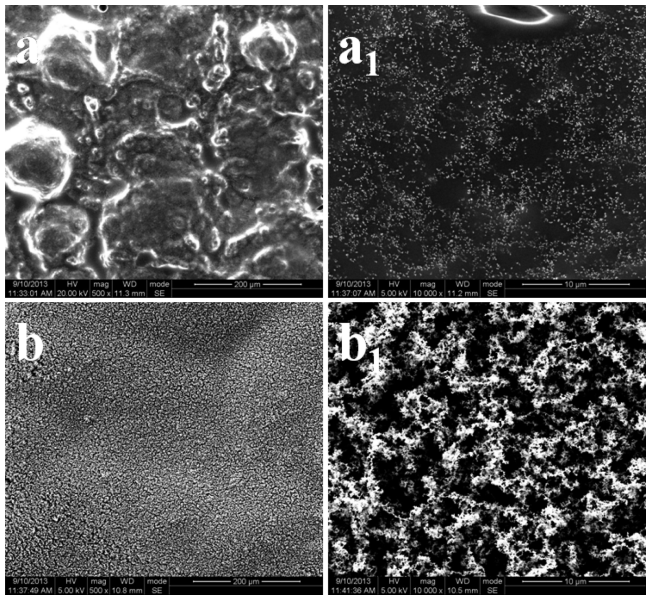

Figure 8. SEM images of PP/APP ((a) ×500, (a_1) ×10000) and PP/PA-APP ((b) ×500, (b_1) ×10000) of the residues obtained from CC tests.

under a N_2 atmosphere. For APP, there are two severe decomposing processes locating at about 296 and 566 °C, respectively. However, for PA-APP, the two severe decomposing processes shifted to 285 and 526 °C, respectively. The thermal decomposing process of APP can be divided into two steps. The first step is in the range of 200-450 °C, the weight loss should be attributed to the elimination of NH_3 and H_2O during the thermal decomposing process of polyphosphate.[26] In this step, the thermal decomposing process of PA-APP is different from that of APP or EDA-APP prepared before,[20] which is more stable than EDA-APP before 270 °C, but less stable than APP. The second step is beyond 450 °C, this weight loss is attributed to the release of phosphoric acid, polyphosphoric acid, and metaphosphoric acid with the decomposition of APP.[26] After incorporating the PA, the MLR of PA-APP was slower than that of APP between 300–400 °C, which might be due to the formation of more char residue at this stage, and these char residue might be the leading effect to the formation of an stable and continuous intumescent char layer in the following stage. To further demonstrate the viewpoint mentioned here, we investigated the condensed phases of PA-APP by FTIR test.

Figure 10 shows the FTIR spectra of the condensed phases at different temperatures. The absorbing peaks at 3400–3030 cm^{-1} could be assigned to the stretching vibration bond of N–H of NH_4^+, indicating the release of ammonia from PA-APP.[24] These peaks decreased gradually, and some of them almost disappeared when the temperature increased to 420 °C. This process was accompanied by the formation of ultra-, pyro- or poly-phosphoric acid due to the production of free acidic hydroxyl groups during the thermal dehydration, as mentioned in our paper.[20] The peaks of P–N–C were observed at 1086 and 723 cm^{-1} with increasing the temperature to about 250 °C. In our previous study,[20] It was well-established that the P–N–C rich char residue could further form the stable residual char, resulting in better flame retardancy. The appearance of P–N–C at about 250 °C demonstrate that the decrease of ML between 300 and 400 °C in TG for PA-APP, compared with APP, should be due to the formation of stable char residue. The absorbing peaks of $-CH_2-CH_2-$ at 2818 and 2754 cm^{-1}

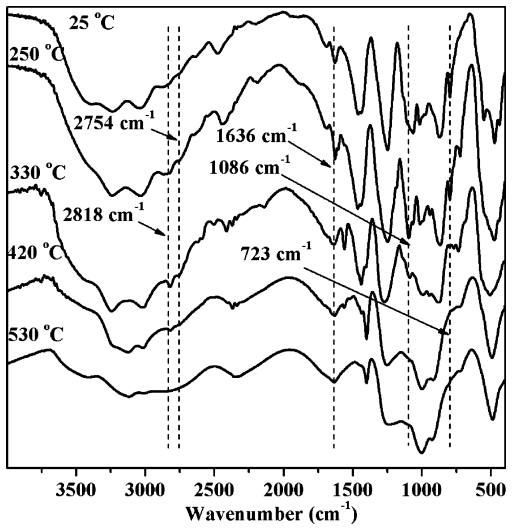

Figure 10. FTIR spectra for the condensed products of PA-APP at different temperatures.

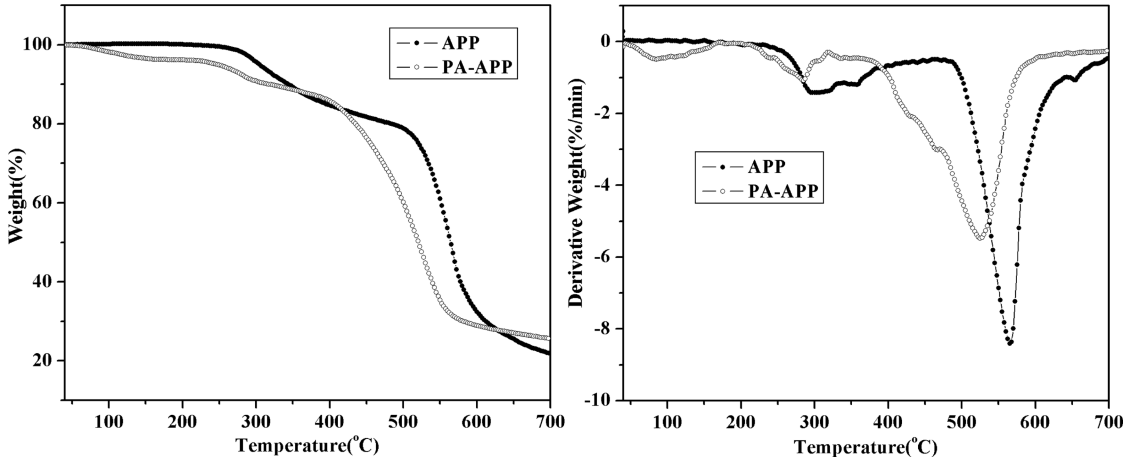

Figure 9. (a) TG and (b) DTG curves of APP and PA-APP at a heating rate of 10 °C/min under a N_2 atmosphere.

disappeared gradually from 250 to 420 °C, and the absorbing peaks at 1636 cm^{-1} become wider, indicating the existence of structures containing C═C.

According to the analysis mentioned above, it can be concluded that the formation of char layer containing P−N−C and C═C etc. could play a positive role in the highly-efficient flame retardancy of PA-APP, in which the production of rich P−N−C must be the leading effect for the formation of better char layer at the later stage.

In addition, XPS data for the condensed products of PA-APP at different temperatures were also utilized to study the flame-retardant mechanism from the viewpoint of elemental change. The changes of the atomic contents of carbon (C), nitrogen (N), oxygen (O), and phosphorus (P) are shown in Table 5.

Table 5. XPS Data of the Condensed Products during the Thermal Decomposition for PA-APP

temp (°C)	C (wt %)	N (wt %)	P (wt %)	O (wt %)
200	43.2	8.1	17.6	31.1
330	45.7	7.5	19.6	27.2
420	30.9	2.1	32.0	35.0
540	30.4	1.9	35.5	32.2

The content of O decreased from 31.1% to 27.2% when the temperature increased to 330 °C from 200 °C, which might be from the condensation dehydration between ammonium salt and P−OH. Then the content of O increased due to the decrease of water release, the release of other gases, and the formation of P−O−P structures. The content of N has the converse change tendency. It kept decreasing with the release of a little NH_3. For the content of C, the release of H_2O and NH_3 resulted in its increase in the condensed phase, subsequently it reduced because of the oxidization of unstable C, and then it increased slightly again because of the formation of stable C structures, such as C═C etc. The content of P maintained increasing from 200 to 540 °C, which should be due to the release of gases and the formation of P−O−P during the thermally decomposing process. Obviously, the change trends for the main elements in the condensed phase are consistent with the thermally decomposing process analyzed in FTIR.

According to the TG, FTIR and XPS tests results, the possible mechanism on charring for PA-APP during the combustion is shown in Scheme 1, and it can be concluded as follows: in the initial stage, along with the release of NH_3 and H_2O, P−N−C structure was formed during the combustion process, so the more stable char residue was formed. Then, with increasing the temperature, part of P−N−C structures decomposed under the catalytic effect of P−OH, accompanied by the release of H_2O and NH_3. Combined with the gas source, most of P−N−C structures and the other stable structures such as C═C, etc., promoted the formation of intumescent, compact, and stable char layer. Finally, the excellent flame-retardant performance of PA-APP was achieved.

4. CONCLUSION

The mono-component polymeric intumescent flame retardant, PA-APP, was prepared successfully. UL-94 vertical burning, OI and CC tests demonstrated tha t PA-APP was much more efficient than APP to flame retard PP. PP/PA-APP composite could pass the UL-94 V-0 rating (3.2 mm) at only 22 wt % flame retardant; meanwhile, its OI value might reach 31.2%.

Scheme 1. Charring Mechanism of PA-APP during the Combustion Process

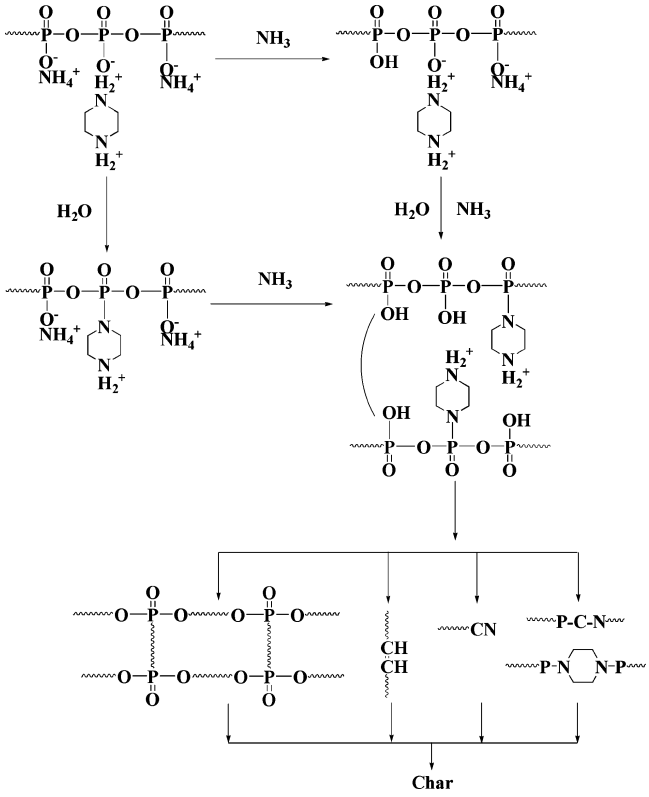

For combustion performance, PP/PA-APP had full range of advantages compared with PP/APP with equal amount of flame retardant, including lower PHRR, lower THR, lower TSP, much lower FGR and PSPR, etc. The study on flame retardant mechanism of PA-APP shows that the P−N−C structure was formed fast at the early stage through the thermal decomposition of piperazine salt (−NH_2−NH_2+P−), consequently could cause the formation of a continuous and compact charlayer, finally led to the better flame retardant performance of PA-APP than APP, so chemically modified PA-APP should be a highly efficient flame-retardant for PP.

AUTHOR INFORMATION

Corresponding Authors

*E-mail: dengcong@scu.edu.cn. Tel. & Fax: +86-28-85410259.
*E-mail: yzwang@scu.edu.cn.

Notes

The authors declare no competing financial interest.

ACKNOWLEDGMENTS

This work was financially supported by the National Natural Science Foundation of China (50933005, 51121001) and Program for Changjiang Scholars and Innovative Research Team in University (IRT1026).

REFERENCES

(1) Wang, Q.; Undrell, J. P.; Gao, Y. S.; Cai, G. P.; Buffet, J. C.; Wilkie, C. A.; O'Hare, D. Synthesis of Flame-Retardant Polypropylene/LDH-Borate Nanocomposites. *Macromolecules.* **2013**, *46*, 6145−6150.

(2) Kwak, S. B.; Nam, J. D. Thermo-Oxidative Stability Study of Polypropylene Composites by Using Cone Calorimetry and Thermogravimetry. *Polym. Eng. Sci.* **2002**, *42*, 1674−1685.
(3) Liu, Y.; Deng, C. L.; Zhao, J.; Wang, J. S.; Chen, L.; Wang, Y. Z. An Efficiently Halogen-Free Flame-Retardant Long-Glass-Fiber-Reinforced Polypropylene System. *Polym. Degrad. Stab.* **2011**, *96*, 363−370.
(4) Liu, Y.; Zhao, J.; Deng, C. L.; Chen, L.; Wang, D. Y.; Wang, Y. Z. Flame-Retardant Effect of Sepiolite on An Intumescent Flame-Retardant Polypropylene System. *Ind. Eng. Chem. Res.* **2011**, *50*, 2047−2054.
(5) Xu, Z. Z.; Huang, J. Q.; Chen, M. J.; Tan, Y.; Wang, Y. Z. Flame Retardant Mechanism of An Efficient Flame-Retardant Polymeric Synergist with Ammonium Polyphosphate for Polypropylene. *Polym. Degrad. Stab.* **2013**, *98*, 2011−2020.
(6) Nachtigall, S. M. B.; Miotto, M.; Schneider, E. E.; Mauler, R. S.; Camargo Forte, M. M. Macromolecular Coupling Agents for Flame Retardant Materials. *Eur. Polym. J.* **2006**, *42*, 990−999.
(7) Yeh, J. T.; Yang, H. M.; Huang, S. S. Combustion of Polyethylene Filled with Metallic Hydroxides and Crosslinkable Polyethylene. *Polym. Degrad. Stab.* **1995**, *50*, 229−234.
(8) Dubois, P. H.; Alexandre, M.; Hindryckx, F.; Jérôme, R. Polyolefin-Based Composites by Polymerization-Filling Technique. *J. Macromol. Sci. Polym. Rev.* **1998**, *38*, 511−565.
(9) Mai, K. C.; Li, Z. J.; Qiu, Y. X.; Zeng, H. M. Mechanical Properties and Fracture Morphology of Al $(OH)_3$/Polypropylene Composites Modified by PP Grafting with Acrylic Acid. *J. Appl. Polym. Sci.* **2001**, *80*, 2617−2623.
(10) Hornsby, P. R.; Watson, C. L. Interfacial Modification of Polypropylene Composites Filled with Magnesium Hydroxide. *J. Mater. Sci.* **1995**, *30*, 5347−5355.
(11) Li, B.; Xu, M. J. Effect of A Novel Charring−Foaming Agent on Flame Retardancy and Thermal Degradation of Intumescent Flame Retardant Polypropylene. *Polym. Degrad. Stab.* **2006**, *91*, 1380−1386.
(12) Wang, J. S.; Wang, D. Y.; Liu, Y.; Ge, X. G.; Wang, Y. Z. Polyamide − Enhanced Flame Retardancy of Ammonium Polyphosphate on Epoxy Resin. *J. Appl. Polym. Sci.* **2008**, *108*, 2644−2653.
(13) Almeras, X.; Le Bras, M.; Hornsby, P.; Bourbigot, S.; Marosi, G.; Keszei, S.; Poutch, F. Effect of Fillers on The Fire Retardancy of Intumescent Polypropylene Compounds. *Polym. Degrad. Stab.* **2003**, *82*, 325−331.
(14) Almeras, X.; Le Bras, M.; Poutch, F.; Bourbigot, S.; Marosi, G.; Anna, P. In Effect of Fillers on Fire Retardancy of Intumescent Polypropylene Blends. *Macromol. Symp* **2003**, *198*, 435−448.
(15) Chiu, S. H.; Wang, W. K. Dynamic Flame Retardancy of Polypropylene Filled with Ammonium Polyphosphate, Pentaerythritol and Melamine Additives. *Polymer.* **1998**, *39*, 1951−1955.
(16) Yang, K.; Xu, M. J.; Li, B. Synthesis of N-Ethyl Triazine-Piperazine Copolymer and Flame Retardancy and Water Resistance of Intumescent Flame Retardant Polypropylene. *Polym. Degrad. Stab.* **2013**, *98*, 1397−1406.
(17) Lu, H. D.; Wilkie, C. A. Study on Intumescent Flame Retarded Polystyrene Composites with Improved Flame Retardancy. *Polym. Degrad. Stab.* **2010**, *95*, 2388−2395.
(18) Hu, X. P.; Li, W. Y.; Wang, Y. Z. Synthesis and Characterization of A Novel Nitrogen − Containing Flame Retardant. *J. .Appl. Polym. Sci.* **2004**, *94*, 1556−1561.
(19) Lv, Q.; Huang, J. Q.; Chen, M. J.; Zhao, J.; Tan, Y.; Chen, L.; Wang, Y. Z. An Effective Flame Retardant and Smoke Suppression Oligomer for Epoxy Resin. *Ind. Eng. Chem. Res.* **2013**, *52*, 9397−9404.
(20) Shao, Z. B.; Deng, C.; Tan, Y.; Chen, M. J.; Chen, L.; Wang, Y. Z. Flame Retardation of Polypropylene via A Novel Intumescent Flame Retardant: Ethylenediamine-Modified Ammonium Polyphosphate. *Polym. Degrad. Stab.* **2013**, DOI: 10.1016/j.polymdegradstab.2013.10.005.
(21) Nie, S. B.; Hu, Y.; Song, L.; He, Q. L.; Yang, D. D.; Chen, H. Synergistic Effect between A Char Forming Agent (CFA) and Microencapsulated Ammonium Polyphosphate on The Thermal and Flame Retardant Properties of Polypropylene. *Polym. Adv. Technol.* **2008**, *19*, 1077−1083.
(22) Camino, G.; Costa, L.; Trossarelli, L. Study of The Mechanism of Intumescence in Fire Retardant Polymers: Part V—Mechanism of Formation of Gaseous Products in The Thermal Degradation of Ammonium Polyphosphate. *Polym. Degrad. Stab.* **1985**, *12*, 203−211.
(23) Breulet, H.; Steenhuizen, T. Fire Testing of Cables: Comparison of SBI with FIPEC/Europacable Tests. *Polym. Degrad. Stab.* **2005**, *88*, 150−158.
(24) Yan, Y. W.; Chen, L.; Jian, R. K.; Kong, S.; Wang, Y. Z. Intumescence: An Effect Way to Flame Retardance and Smoke Suppression for Polystryene. *Polym. Degrad. Stab.* **2012**, *97*, 1423−1431.
(25) Katsoulis, C.; Kandare, E.; Kandola, B. K., Thermal and Fire Performance of Flame-Retarded Epoxy Resin: Investigating Interaction between Resorcinol Bis (Diphenyl Phosphate) and Epoxy Nanocomposites. Hull, T. R., Kandola, B. K., Eds.; Royal Society of Chemistry: Cambridge, U.K., 2009; Chapter 17, pp 184−205.
(26) Liu, G. S.; Chen, W. Y.; Yu, J. G.; Novel, A. Process to Prepare Ammonium Polyphosphate with Crystalline Form II and its Comparison with Melamine Polyphosphate. *Ind. Eng. Chem.Res.* **2010**, *49*, 12148−12155.